Active optical control of the terahertz reflectivity of high-resistivity semiconductors

L. Fekete, J. Y. Hlinka, F. Kadlec, and P. Kužel

Institute of Physics, Academy of Sciences of the Czech Republic, Na Slovance 2, 182 21 Prague 8, Czech Republic

P. Mounaix

Centre de Physique Moléculaire Optique et Hertzienne, Université Bordeaux I, 351 Cours de la Libération,
33405 Talence Cedex, France

Received February 7, 2005

We study theoretically and demonstrate experimentally light-controllable terahertz reflectivity of high-resistivity semiconductor wafers. Photocarriers created by interband light absorption form a thin conducting layer at the semiconductor surface, which allows the terahertz reflectivity of the element to be tuned between antireflective ($R<3\%$) and highly reflective ($R>85\%$) limits by means of the intensity and wavelength of the optical illumination. © 2005 Optical Society of America

OCIS codes: 160.5140, 310.6860, 300.6270, 300.6500, 230.1150, 230.4110.

Generation and control of pulsed and continuous-wave terahertz (THz) radiation have received considerable attention in the past few years.[1–3] As more-efficient THz sensors and sources become available, there will be increasing research emphasis on manipulation of freely propagating THz beams for future technology. Particular emphasis should be placed on all-optical devices that allow transfer of information from the optical spectral band to the THz band, opto-THz switches, and modulators.

High-resistivity semiconductors show a big potential for opto-THz coupling. On the one hand, in their ground state they are transparent and virtually dispersion free for THz radiation. On the other hand, photoexcited semiconductors exhibit a strong interaction with THz light mediated by free carriers. Fine tuning of the strength of the interaction by the intensity of optical excitation then leads to interesting phenomena that are directly utilizable for THz-light modulation and switching.

Kröll *et al.*[4] recently demonstrated a metallic antireflection coating for the THz range by deposition of a thin chromium layer onto a THz sensor. In this Letter we show theoretically and demonstrate experimentally that a thin photoexcited layer at the surface of a semiconductor wafer can exhibit similar properties. In addition, the thickness of such a layer and its complex refractive index in the THz range can be tuned by variation of the wavelength and the intensity of the optical illumination. Both antireflective and highly reflective regimes can then be easily achieved and used to modulate the amplitude or phase of the THz radiation efficiently.

For a theoretical model, let us consider a structure consisting of three media with plane-parallel interfaces: (i) a lossless low-impedance medium (denoted by subscript 0) filling the half-space of the incident wave (in our case it is an undoped semiconductor in the ground state), (ii) a thin conductive layer with thickness d_1 (subscript 1), representing the photoexcited part of the semiconductor, (iii) and finally, a half-space containing the transmitted wave filled with a lossless high-impedance medium, e.g., air in our case. The THz refractive indices of these media are $N_0=n_0$, $N_1=n_1-i\kappa_1$, and $N_2=1$, respectively. The reflection of the THz radiation on this structure (assuming sharp plane-parallel interfaces) is described by amplitude reflection coefficient r, defined as[5]

$$r=\frac{r_{12}\exp(-2i\omega N_1 d_1/c)-r_{10}}{1-r_{10}r_{12}\exp(-2i\omega N_1 d_1/c)}, \tag{1}$$

where c is the speed of light in vacuum, ω is the probing THz angular frequency, and r_{10} and r_{12} are the Fresnel amplitude reflection coefficients describing internal reflections within the photoexcited layer. In our approximation, d_1 is assumed equal to the penetration depth of the optical pump beam in the semiconductor. Complex refractive index N_1 depends on the wavelength and intensity of the optical excitation. For simplicity, Eq. (1) assumes normal incidence of the probing radiation (i.e., that angles of incidence α_i in the three media are all equal to 0). However, if d_1 is replaced by $d_1\cos\alpha_1$ in Eq. (1) and throughout this Letter, expressions for an arbitrary angle of incidence can easily be obtained.

When the photoexcited sheet is thin enough, i.e., when $|N_1|\ll c/(2\omega d_1)$, which can be achieved at low optical pump fluences, it may act as an antireflective layer for the THz (probing) wave. Indeed, the numerator of Eq. (1) vanishes for

$$N_1\approx\left[\frac{(n_0-1)c}{2\omega d_1}\right]^{1/2}(1-i). \tag{2}$$

The problem can also be considered in analogy with the theory of electrical circuits. The photoexcited layer plays the role of a shunting impedance Z_1, improving the impedance mismatch between the bulk semiconductor and the air. The thin-layer condition described above means that d_1 is much smaller than the skin depth of the photoexcited sheet in the THz range. It follows[6] that $Z_1=1/(d_1\sigma_1)$, where σ_1 is the THz conductivity of the photoexcited sheet and im-

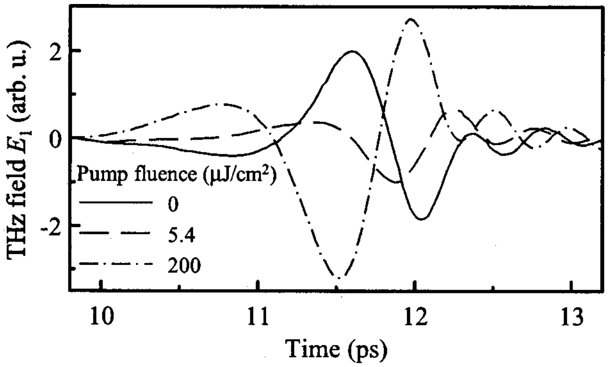

Fig. 1. THz waveforms internally reflected at the photoexcited surface of a GaAs wafer for several pump pulse fluences at 810 nm.

pedance matching condition $1/Z_1 = 1/Z_0 - 1/Z_2$ reads as

$$d_1\sigma_1 = \sqrt{\epsilon_0/\mu_0}(n_0 - 1), \tag{3}$$

where ϵ_0 and μ_0 are the permittivity and the permeability of vacuum, respectively. It is then straightforward to show that conditions (2) and (3) are equivalent.

In the THz spectral range, the optical properties of photoexcited semiconductors with free-carrier densities not exceeding 10^{18} or 10^{19} cm^{-3} can usually be well described by the Drude model. The behavior of the complex THz refractive-index versus carrier density is then characterized by a crossing of n_1 and κ_1 in the range 10^{15} to 10^{17} cm^{-3} for most common semiconductors, such as GaAs, InP, and Si. The values of the crossing can be quite close to those required by condition (2), depending on the optical and THz frequencies used.

If the incident optical fluence is further increased and the photocarrier density reaches sufficiently high values that $\kappa_1 > c/(2\omega d_1)$, the exponential terms in Eq. (1) can be neglected and the probing wave will undergo reflection on a thick conductive sheet, yielding reflection coefficient r close to unity.

For the experiments we used a Ti:sapphire multipass amplifier delivering 1 mJ pulses with a duration of 55 fs and a mean wavelength of $\lambda = 810$ nm at a repetition rate of 1 kHz. One part of the beam was used for the sample excitation; its intensity was varied using a pair of gradient neutral-density filters. Another part of the beam was used for the generation and detection of THz pulses in our time-domain THz setup.[7,8] We studied semi-insulating 0.35 mm GaAs and 0.26 mm thick Si wafers. The sample was fixed to a circular aperture with a diameter of 3 mm, which was placed after the sample. The pump beam excited a surface area with a diameter of 5 mm, which was larger than that contributing to the measured THz signal.

To record the reflectance spectra of the photoexcited sample we employed the configuration described in Ref. 7. Briefly, a probe THz pulse is incident onto the input surface of an unexcited semiconductor, and it propagates through the sample without attenuation toward the output surface. Subsequently, when the entire THz probe pulse is inside the sample, the input surface is optically excited by a femtosecond pump pulse. The part of THz pulse $E_0(t)$ that is directly transmitted through the output face is used as a reference. The part reflected on the output surface propagates back to the photoexcited input face, reflects from its inner side, and is detected as the first echo, $E_1(t)$. It serves as an internal reflectance probe. The complex reflectance spectrum of the photoexcited surface is then equal to

$$r(\omega) = \frac{E_1(\omega)}{r_0 E_0(\omega)}, \tag{4}$$

where r_0 is the amplitude reflection coefficient of the unexcited GaAs surface.

Examples of reflected waveforms E_1 for three different pump fluences are shown in Fig. 1. The reference waveforms E_0 (not shown) are identical for the three measurements. The variations of both amplitude and phase of the reflection coefficient in the antireflective (dashed curve) and in the highly reflective (dashed–dotted curve) regimes are clearly identified. The tuning curves of the THz reflectance versus pump intensity for selected THz frequencies are shown in Fig. 2. The theoretical reflectance curves were calculated using a numerical approach described in Ref. 9. We assumed a linear absorption regime with a negligible carrier diffusion on a time scale of picosecond pump–probe delays, i.e., an expo-

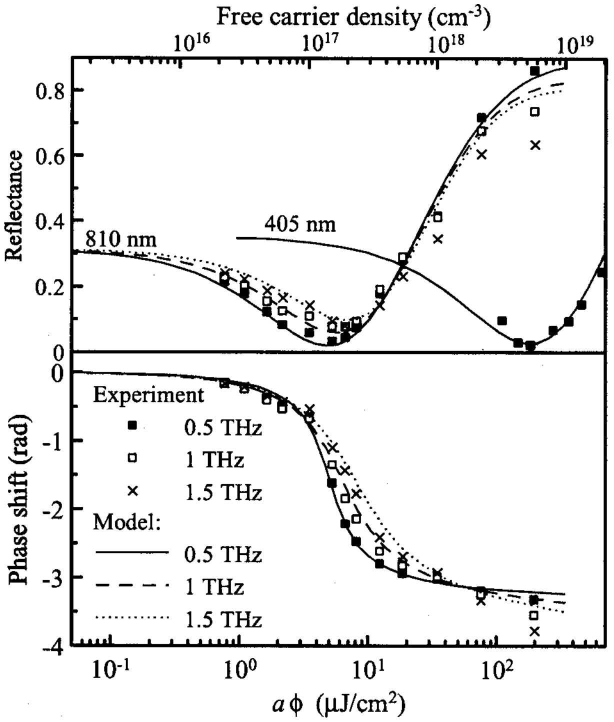

Fig. 2. Power reflectance and phase change of the internally reflected THz wave versus incident optical pump fluence ϕ and the corresponding free-carrier density for two optical wavelengths ($a=1$ for 810 nm and $a=0.5$ for 405 nm) in GaAs.

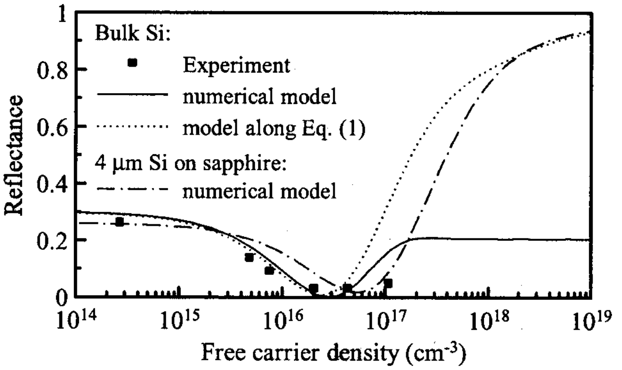

Fig. 3. Internal power reflectance at 0.5 THz for Si optically excited at 810 nm. Bulk sample, $d_1=10.6$ μm; thin film, $d_1=4$ μm.

nential decrease of the free-carrier density along the surface normal. We took into account the interaction of the THz radiation with both electrons and heavy holes; their contribution to the optical constants was described using the Drude model.[5] This model fits the experimental data well, with the exception of the highest pump fluences. In GaAs, for these fluences ($\phi \gtrsim 70$ μJ cm^{-2}), nonlinear optical absorption processes such as two-photon absorption and saturation of single-photon absorption occur.[7] A sign of these effects is the phase shift upon reflection, which reaches values clearly below $-\pi$ owing to an increase of the photoexcited layer's thickness.

The simple analytical model introduced above provides a clear insight into the underlying physics of the problem. However, its validity is expected to be limited due to the gradient of the photoexcited carrier density along the surface normal. We found that the analytical model is in semiquantitative agreement with the numerical calculation. It significantly differs from the numerical model only for very high carrier densities and for large values of d_1 (low absorption of the pump pulse). In both these cases a relatively thick zone with a slowly variable carrier density builds up where efficient absorption of the THz radiation occurs. The analytical model then overestimates the reflectance intensity (as discussed below).

We studied the influence of layer thickness d_1 (which is related to the pump pulse's wavelength) on the THz properties of the structure. Assuming a Drude behavior of the photoexcited carriers, relation (2) can be solved analytically. It follows that for free carriers with properties similar to those in GaAs the ideal thickness for the antireflective regime is ~ 10 μm (i.e., excitation close to the bandgap edge).

However, for such a layer thickness the relatively low gradient of the free-carrier density leads to significant absorption of the probing THz radiation at high carrier concentrations; consequently, the high-reflectivity regime cannot be achieved.

Similar behavior is expected when the diffusion process of free carriers plays a role, as in the case of silicon, for which the carrier lifetime is long.

The free-carrier lifetime in our Si sample was approximately 0.3 to 0.4 ms, which is close to the repetition rate of the optical pulses. The effect is illustrated in Fig. 3: For high free-carrier concentrations the results of the analytical model differ significantly from those obtained with the numerical model, which predicts the experimental values better. The difference between the experimental results and the numerical model is due to carrier diffusion, which is not taken into account by our model. In principle, the high-reflectivity regime can be restored using semiconductor films deposited on insulating transparent substrates, such as silicon on sapphire. In this case the diffusion is suppressed and d_1 is defined by the layer's physical thickness (dashed–dotted curve in Fig. 3).

For the frequency range where the optical pulse is strongly absorbed ($d_1 \ll 1$ μm), the reflectance tuning curve is significantly shifted toward high photocarrier densities, which may be hard to achieve. For example, Fig. 2 shows the lower part of the tuning curve for the optical pumping at 405 nm. The penetration depth for this wavelength is ~ 17 nm, and the tuning curve is shifted by ~ 2 orders of magnitude with respect to that for the 810 nm pump wavelength.

One can conclude that a very good choice consists in using moderate penetration depths (~ 1 μm)—as shown in Fig. 2 for a 810 nm pump—or thick films (several micrometers) on transparent substrates. In both cases a high modulation depth of the reflectance is obtained.

In summary, we have demonstrated the possibility of optical tuning of complex THz reflectance at semiconductor surfaces. In GaAs, we achieved outstanding modulation of the reflected THz wave ($R=3\%$ to 85%) by means of both laser pump intensity and wavelength switching.

Financial support by the Academy of Sciences of the Czech Republic (project 1ET300100401) and by its grant agency (project KJB100100512) is acknowledged. P. Kužel's e-mail address is kuzelp@fzu.cz.

References

1. M. C. Nuss and J. Orenstein, in *Millimeter and Submillimeter Wave Spectroscopy of Solids*, G. Grüner, ed., Vol. 74 of Topics in Applied Physics (Springer-Verlag, 1998), Chap. 2, pp. 7–50.
2. D. Mittleman, *Sensing with Terahertz Radiation* (Springer-Verlag, 2003).
3. B. Ferguson and X.-C. Zhang, Nat. Mater. **1**, 26 (2002).
4. J. Kröll, J. Darmo, and K. Unterrainer, Electron. Lett. **40**, 763 (2004).
5. M. Born and E. Wolf, *Principles of Optics*, 7th ed. (Cambridge U. Press, 2003).
6. J. D. Jackson, *Classical Electrodynamics* (Wiley, 1998).
7. F. Kadlec, H. Němec, and P. Kužel, Phys. Rev. B **70**, 125205 (2004).
8. P. Kužel and J. Petzelt, Ferroelectrics **239**, 949 (2000).
9. R. Jacobsson, in *Progress in Optics*, E. Wolf, ed. (North-Holland, 1965), Chap. 5, pp. 255–258.